Measurement of the Branching Ratio b→ $\ell\nu X$ with Electrons, Muons and Neutrinos

The L3 Collaboration

Abstract

The inclusive branching ratio BR(b→ $\ell\nu X$) has been measured by identifying electrons, muons and neutrinos in a sample of well measured 2–jet hadronic Z decays. The obtained results for the branching ratios are (10.89±0.20±0.51)% and (10.82±0.15±0.52)% for electrons and muons, respectively. The branching ratio obtained with neutrinos includes the decays b→ $\tau\nu X$. Assuming that the different semileptonic b–decay rates are produced in the ratio e:μ:τ of 1:1:0.25(±0.05), the branching ratio $b \to \nu X$ is found to be (23.08±0.77±1.24)%, corresponding to a BR($b \to e(\mu)\nu X$) of (10.26±0.35±0.55)%. Combining the three BR measurements and taking correlations into account the BR(b→ $e(\mu)\nu X$) is measured to be (10.73±0.11±0.46)%. Alternatively, constraining the contributions from electrons and muons to the direct measurement, we obtain a neutrino excess, attributed to the decay b→ $\tau\nu X$, with a BR of (1.67±0.46±1.04)%. The ratio BR(b→ $\tau\nu X$)/BR(b→ $e\nu X$) is (0.154±0.042±0.070), in agreement with theoretical expectations.

submitted to the EPS conference, Brussels 1995

and the Lepton–Photon conference, Beijing 1995

1 Introduction

The semileptonic branching ratio BR $(b \to \ell\nu X)$ is an important quantity for understanding the weak decay dynamics of heavy flavored hadrons. Measurements of the BR are usually done with identified electrons and muons. However, this BR can also be measured with neutrinos, using the missing energy spectrum of jets, obtained indirectly using the difference between the kinematically constraint jet energy, assumed to be the beam energy, and the measured jet energy ($E_\nu \approx E_{beam} - E_{jet}$). The BR measurement with energetic neutrinos is complementary to the traditional BR measurements with inclusive electron and muons, as it is sensitive to the assumed polarization of the virtual W in b–hadron decays and to the BR(b$\to$ $\tau\nu X$). Furthermore, the systematic error due to backgrounds and efficiencies are different from the measurements with electrons and muons. The neutrino analysis is restricted to "two–jet" events since the expression for the neutrino energy is not valid for hard three–jet events. In order to compare the neutrino BR measurement with the direct BR results with electrons and muons, all measurements are done for the same sample of hadronic two–jet Z decays. This is different from previous measurements from L3, where the entire hadronic event sample was used [1].

For this BR measurement, the fraction of b–flavored hadronic Z decays has been constrained to the Standard Model value of 21.6%. The measurements of the semileptonic BR$(b \to \ell\nu X)$ with inclusive electrons, muons and neutrinos in hadronic Z decays are discussed. The measurement is performed with the L3 experiment at LEP described in detail in [2], with the data collected during the 1991 and 1992 data taking periods.

2 Event selection

For this analysis only the events taken within ± 0.5 GeV of the Z peak are used. The hadronic events are selected with the criteria described in [3]. As the BR analysis for each studied channel is limited by systematic uncertainties, it is further required that the hadronic events are well contained in the hermetic barrel region of the detector. The following additional selection criteria are used:

- The visible energy in each hemisphere, defined by the thrust axis of the event, must be larger than 10% of the beam energy.
- The polar angle $\theta_{\rm H}$ of the momentum vector sum of all calorimeter clusters associated with each hemisphere has to fulfill the condition $|\cos\theta_{\rm H}| < 0.7$. For the BR measurements only jets which satisfy the condition $|\cos\theta_{\rm H}| < 0.65$ are considered.
- The energy sum of all calorimeter clusters with $|\cos\theta| > 0.74$ is smaller than 5 GeV.
- If the visible energy of the event is smaller than 70% of the beam energy, then the missing transverse energy of the event must either be larger than 50% of the beam energy or larger than the missing longitudinal energy.
- The number of charged tracks must be larger than four and at least three tracks each with a transverse momentum with respect to the beam of more than 150 MeV and a distance of closest approach smaller than 1 mm have to be found in at least one hemisphere.

A total of 402k hadronic events, are selected with these criteria. A geometrical cone algorithm is used to form jets out of the calorimeter clusters. Using this jet definition, the events are divided into "two–jet" and "three–jet" events. Events are classified as two–jet events if there are either two such jets in the event, or if the invariant mass of all jets found in a hemisphere is less than 25 GeV. With this selection, 346k events are classified as two–jet events.

Monte Carlo events are simulated using JETSET [4] and a GEANT based description of the L3 experiment [5]. Weak decays of c– and b–hadrons are simulated such that the measured inclusive charged lepton spectra and the branching ratios for charm and beauty decays [6] are reproduced. The simulated energy spectra of electrons, muons and neutrinos agree also with the inclusive lepton spectra obtained for b–hadron decays from the ACCM model [7]. More details about the simulation of weak decays of c– and b–flavored hadrons are given in [8].

For this study the energy spectra of the primary b–hadrons[1] are simulated with the Peterson function [9] as implemented in the JETSET framework. It is tuned such that the average energy of the weakly decaying b–hadrons (B_d, B_u, B_s and Λ_b) corresponds to 72% of the beam energy. With this simulation for the b–hadron energy spectrum, good agreement between the data and the Monte Carlo is obtained for the electron, the muon and the simultaneously measured neutrino energy spectra [8]. Using the same analysis chain as for the data, 497k fully simulated Monte Carlo events remain after the barrel event selection, out of which 424k events are classified as two–jet events. The fraction of b–flavor events in this subsample is found to increase, due to the removal of hard three–jet events, from the generated 21.6% in the overall Monte Carlo sample to 22.8% in the two–jet sample.

2.1 Selection of b–enriched and depleted event subsamples

For our analysis we also select four different event subsamples (I–IV) which have either enhanced or depleted b–fractions.

A lifetime based selection of b–flavored enriched and depleted event subsamples proceeds as follows. The events are separated into two hemispheres defined by the thrust axis of the event which is measured from the reconstructed calorimeter clusters. A secondary vertex per hemisphere is obtained using well measured tracks with a transverse momentum with respect to the beam of more than 500 MeV. The events which have a large distance between the two reconstructed vertices are selected as candidates for b–flavored events.

The accepted tracks are used to determine a secondary vertex with the b–hadron flight direction, which is approximated with the thrust axis of the event. The average value of these track vertices per hemisphere is used, weighting each track with the measured p_t with respect to the thrust axis of the event. If more than three tracks are accepted per hemisphere, the three tracks with the largest distances are used to estimate the secondary vertex per hemisphere. The distance with respect to the fill vertex is assumed to be zero if no track is accepted. To be essentially independent from the beam spot determination, the distance between the two reconstructed hemisphere vertices is used to select b–flavored events. The measured distance

[1]The production of B^{**} particles was not taken into account.

distributions for the data and the Monte Carlo are shown in figure 1. The expected distance distribution from b–flavored Monte Carlo events is also shown.

Events which have a distance between the two vertices of more than 3.5 mm define the b–flavor enriched sample I. Using the efficiencies from the Monte Carlo simulation for b–flavored events and backgrounds, the b–flavor purity of the sample is found to be 60.8%. The error on this purity due to uncertainties in the tracking simulation and the production and decays of c– and b–flavored hadrons are found to be larger than that from experimental uncertainty in $R_{b\bar{b}}$ [10].

Since this b–flavor enriched event sample I will mainly be used to measure BR(b$\rightarrow \nu X$), the uncertainty in the b–flavor purity can be reduced using the Standard Model value for $R_{b\bar{b}}$ of 21.6% and the requirement that the measured BR's using electron and muon candidates with high p and p_t (section 3), agree for the two–jet events and the lifetime tagged events (subsample I). With this constraint, the purity of b–flavored events in subsample I is found to be 59.4$\pm$1.5%. The uncertainty in the purity comes mainly from the error on the BR's obtained with high p and p_t electron and muon candidates (sections 3.1 and 3.2).

The lifetime based event classification is also used to obtain a b–flavor depleted sample. Events with a reconstructed negative decay distance between the two hemispheres are used to define sample II, with a remaining b–flavor fraction from the Monte Carlo simulation of 11%.

Event sample III is selected with the requirement that a high $x(= E_i/E_{beam})$ particle i is found in at least one jet. It is required that either a high momentum track with a momentum above 60% of the beam energy and an associated calorimeter cluster of more than 50% of the beam energy, or an energetic π^0 candidate with an energy above 50% of the beam energy is found in one jet. The jet found in the hemisphere opposite to the one containing the high x particle defines this light quark–flavor enriched jet sample. According to the Monte Carlo, the remaining b–flavor fraction is 10% in this sample.

A further b–enriched jet sample (IV), with a b–flavor fraction of 83% is obtained from jets which are found opposite to jets with a high p and p_t charged lepton with respect to the jet direction.

2.2 Selection of inclusive electron candidates

Electron candidates are selected with the following criteria:

- The energy of a cluster E_{BGO} in the barrel BGO calorimeter (with the polar angle θ $|\cos\theta| < 0.72$) must be larger than 3 GeV. The hadronic calorimeter energy associated with this cluster must be smaller than 2 GeV.
- Between 10 and 40 crystals are associated with the BGO–cluster and that more than 95% of the energy is deposited in the central 9 crystals.
- One charged track must point to this BGO cluster and the difference between the azimuthal angle estimated from the shower center and the estimated track impact point at the BGO calorimeter is smaller than 4 mrad + 8 mrad$/E_{BGO}$ (in GeV).

- The measured p_t with respect to the beam direction for the charged track is consistent (within 3 σ) with the p_t measurement from the BGO calorimeter.

With this selection, 8184 (5338 with a p_t of more than 1.4 GeV with respect to the jet direction) electron candidates are selected in the two–jet event sample.

2.3 Selection of inclusive muon candidates

Muon candidates are selected using the following criteria:

- Tracks found in the barrel muon system must be reconstructed in at least two out of the three ϕ–layers and one out of the two possible z–chamber layers.
- The distance of closest approach to the event vertex in the transverse plane, extrapolated taking the errors due to multiple scattering into account, has to be smaller than 100 mm. This distance must also be smaller than three times the estimated distance error due to multiple scattering in the calorimeters.
- The measured $\mu^{\pm}$ momentum must be larger than 4 GeV.

With this selection 24182 (9809 with a p_t of more than 1.4 GeV with respect to the jet direction) muon candidates are selected in the two–jet event sample.

2.4 Selection of jets with inclusive neutrino candidates

The visible energy spectrum of jets containing semileptonic b–decays from the Monte Carlo is shown in figure 2a. The contributions from the decays b$\rightarrow e\nu X$, b$\rightarrow \mu\nu X$ and b$\rightarrow \tau\nu X$, including the subsequent charm–hadron and τ decays, are shown separately. The visible energy spectra of jets associated with the decays b$\rightarrow e\nu X$ and b$\rightarrow \mu\nu X$ are slightly different. The reason is that undetected muons increase the missing energy, while the energy from unidentified electrons is still measured in the calorimeter. The Monte Carlo visible energy distribution for generic b–flavored jets is shown in figure 2b. As can be seen from the hatched histogram, jets associated with semileptonic b–decays dominate the region of jets with large missing energy. In the Monte Carlo one finds that for 100% b–flavored jets and the requirement that the missing energy of a jet is larger than 15 GeV, about 82% of the jets originate from semileptonic b–decays. In the generic Monte Carlo two–jet event sample about 50% of the jets with a missing energy of more than 15 GeV originate from semileptonic b–decays.

In order to use the missing energy signature of jets to measure BR(b$\rightarrow \nu X$), uncertainties in the backgrounds from mismeasured jets must be reduced as much as possible. For this measurement the b–flavor enriched event sample I is used.

The energy measurement for jets with large missing energy due to mismeasured jets is compared in the data and Monte Carlo using the b–flavor depleted samples (II and III). While the mean jet energy values are well described, the jet energy resolution is about 10% smaller in the data than in the Monte Carlo. The Monte Carlo also underestimates the number of jets with large missing energy by roughly 15%.

3 Measurement of the BR (b→ $\ell\nu X$)

The semileptonic BR($b \to \ell\nu X$) for electrons, muons and neutrinos are obtained using the relation:

$$BR = \frac{n_\ell - n_{back}}{\epsilon \times N_{b-jets}}, \tag{1}$$

where n_ℓ is the number of observed lepton candidates, n_{back} is the number of background events, ϵ is the efficiency and N_{b-jets} is the number of selected b–jets. The number of b–jets is obtained from the Monte Carlo simulation for the used event sample, starting with the Standard Model value for $R_{b\bar{b}}$ of 21.6%. Using alternatively the experimental average value of (22.02±0.2)% for $R_{b\bar{b}}$ [10], all results for the BR's would decrease by (2±1)% relative.

To enhance the fraction of semileptonic b–decays, a high value for the p_t of the electrons and muons with respect to the jet direction is used. To reduce ambiguities from the jet definition, we use all energy clusters, beside the lepton candidate, which are found in the same hemisphere as the charged lepton candidate, to define the jet. The charged lepton p_t is calculated with respect to this jet direction.

The BR's are measured using the two–jet event sample and demanding electron and muon candidates with high p_t (more than 1.4 GeV) with respect to the closest jet. For an estimate of the systematic error due to the event selection, the p_t and the two–jet event definitions are varied. The simulation of b–decays agrees with the spectra expected from the ACCM model. Using a softer charged lepton spectrum for the efficiency determination, as for example obtained with the ISGW model [11], relative BR changes of about 3–4% have been found previously [12]. Since these b–model uncertainties are strongly correlated with the uncertainties in the b–hadron fragmentation function and the b–hadron p_t spectrum, they are included in the systematic errors obtained with the lepton p and p_t spectra.

3.1 BR measurement with electrons

The p_t spectrum for electron candidates with a momentum above 3 GeV is shown in figure 3a for the data and the Monte Carlo, normalized to the number of selected hadronic events. For low p_t values about 30% more electron candidates are found in the data than in the Monte Carlo. A similar excess of low p_t electron candidates is found in the b–flavor depleted event samples, II (shown in figure 3b) and III. There is no excess seen in the b–enriched sample I. Therefore it can be concluded that the Monte Carlo underestimates the electron background in the low p_t regions.

For larger p_t values of the electron candidates one finds good agreement between the data and the Monte Carlo for the different subsamples. The momentum spectra for the electron candidates with a p_t between 1.4–2.1 GeV and above 2.1 GeV are shown in figure 4a and b. The fraction of electron candidates per hadronic event in the data and the Monte Carlo for different p_t values and the resulting BR values are given in table 1. The corresponding numbers for the high p_t electron candidates are also separated for the two years of data taking and for the different b–flavor enriched and depleted event subsamples. For sample III the fractions of high p_t electrons and muons (section 3.2) per tagged jet are much lower in the data than in the Monte Carlo. This anomaly is probably related to a different b–flavor content of sample III in the data than in the Monte Carlo, as discussed in section 4.

	Data	Monte Carlo		Data
p_t (GeV)	$n_{e^\pm}/n_{had} \times 10^3$	$n_{e^\pm}/n_{had} \times 10^3$	purity $b \to e^\pm \nu X$ [%]	BR[%]
0.0–0.7	2.093±0.077	1.543±0.060	28.5	9.55±1.28
0.7–1.4	6.135±0.133	5.979±0.12	48.3	11.01±0.32
1.4–2.1	6.108±0.132	6.040±0.12	73.3	10.61±0.31
>2.1	9.323±0.164	8.916±0.15	78.3	11.05±0.27
> 1.4	15.432±0.211	14.957±0.19	76.3	10.89±0.20
> 1.4 (91)	15.835±0.413	15.363±0.20	76.3	10.85±0.30
> 1.4 (92)	15.285±0.246	14.754±0.20	76.3	10.93±0.22
> 1.4 (I)	33.83±0.91	33.73±0.82	87.5	10.48±0.47
> 1.4 (II)	8.50±0.30	8.70±0.27	64.0	10.08±0.48
> 1.4 (III)	3.30±0.31	3.98±0.34	57.9	7.4±1.0
> 1.4 (IV)	23.4±1.2	24.8±1.2	89.0	9.8±0.7

Table 1: Number of electron candidates per hadronic event in the data and in the Monte Carlo. For the Monte Carlo the estimated purity of correctly identified semileptonic b–decays with an input BR of 10.45% is also given. The corresponding numbers for the various subsamples (I–IV) are also given.

For p_t values of less than 0.7 GeV, where a significant difference between the data and the Monte Carlo is observed, a correction for the Monte Carlo background estimate can be applied. Assuming that the background is underestimated by the excess observed in the low p_t region of the b–flavor depleted event samples II and III, a corrected BR value of (9.55±1.28(stat.)) is obtained.

The contributions to the systematic uncertainties in the BR measurement are listed in table 2. The systematic error from the background and efficiency are estimated from the difference of the BR's from the two highest p_t bins, with respect to the average BR value. The uncertainty due to the detector simulation have been studied using a variations in the selection criteria.

Uncertainties related to the b–hadron energy spectrum are estimated using the agreement between the observed electron p spectrum in the data and in the Monte Carlo. One finds that the observed electron p spectra for the different p_t bins are described by the Monte Carlo with an average energy spectrum of $X_E = 0.72 \pm 0.02$ for the weakly decaying b–hadrons, corresponding to a BR error of $\mp 0.2\%$. Uncertainties from c–decays have been estimated from a relative variation of ±10% for the background from semileptonic c–hadron decays. We have also varied the two–jet definition for the event selection and find that uncertainties due to the simulated b–hadron p_t spectrum result in an additional uncertainty of $\pm 0.3\%$. More details about this study are given in section 4.

error source	Δ BR(b$\rightarrow e\nu X$)	Δ BR(b$\rightarrow \mu\nu X$)
selection efficiency	0.13	0.20
background p_t criteria	0.28	0.31
semileptonic c–hadron decays	0.13	0.26
b–hadron E spectrum ($< X_E >= 0.72 \pm 0.02$	0.25	0.25
two–jet definition	0.29	0.04
combined error	0.51	0.52

Table 2: Estimated contributions to the systematic error for the BR measurement with high p_t inclusive electron and muon candidates.

After applying the corrections for the background, the BR(b$\rightarrow e\nu X$) measured with the inclusive electron candidates and a p_t of more than 1.4 GeV, adding the systematic errors in quadrature, is $10.89 \pm 0.20\% \pm 0.51\%$.

3.2 BR measurement with muons

The p_t spectrum with respect to the jet for the muon candidates with a momentum above 4 GeV is shown in figure 5a for the data and the Monte Carlo, normalized to the number of selected hadronic events. The p_t spectrum of the inclusive muon candidates is well described by the Monte Carlo. Furthermore, good agreement between the data and the Monte Carlo is also found for the p_t spectra in the b–flavor enriched and b–flavor depleted event subsamples I–IV. For example, the p_t spectrum for the muon candidates in sample II is shown in figure 5b. One concludes that the backgrounds are accurately described by the Monte Carlo. The momentum spectra of the muon candidates with a p_t between 1.4–2.1 GeV and more than 2.1 GeV are shown in figure 6a and b.

The fraction of muon candidates per hadronic event found in the data and in the Monte Carlo for different p_t bins and the different event subsamples are given in table 3.

The systematic error on the BR has been estimated from the different sources listed in table 2. The background and geometrical efficiency uncertainties are estimated using the observed angular distribution of muons in the data and Monte Carlo. The inefficiency of the muon chamber system for the data with respect to the Monte Carlo description has been estimated to be $5 \pm 1.5\%$ for the 1992 data and about $3\% \pm 1\%$ for the 1991 data. These estimates agree within the errors with the independent studies performed with $\mu^+\mu^-$ pairs. The difference in the BR results for p_t values between 1.4–2.1 GeV and for larger p_t values with respect to the average is taken as the systematic error of the background and signal efficiency. A further uncertainty from the simulation of the fragmentation function of the weakly decaying b–hadrons with an average X_E of 0.72 ± 0.02 results in a systematic error of $\mp 0.25\%$. From a variation of the two–jet definition for the event selection, described in more detail in section 4, the uncertainties due to the simulated b–hadron p_t spectrum correspond to a further uncertainty of $\pm 0.04\%$.

After correcting for backgrounds and efficiency, a BR(b$\rightarrow \mu\nu X$) of (10.82±0.15±0.52)% is obtained using muons with a p_t above 1.4 GeV.

	Data	Monte Carlo		Data
p_t (GeV)	$n_{\mu^\pm}/n_{had} \times 10^3$	$n_{\mu^\pm}/n_{had} \times 10^3$	purity $b \rightarrow \mu^\pm\nu X$ [%]	BR[%]
0.0–0.7	21.087±0.246	21.363±0.224	9.2	9.88±0.42
0.7–1.4	20.466±0.243	20.986±0.222	29.3	9.57±0.15
1.4–2.1	12.457±0.189	12.413±0.171	61.8	10.51±0.22
$>$ 2.1	15.901±0.214	15.292±0.189	71.2	11.03±0.20
$>$1.4	28.359±0.286	27.706±0.255	67.0	10.82±0.15
$>$1.4 (91)	29.314±0.562	28.073±0.255	67.0	11.1±0.3
$>$1.4 (92)	28.016±0.333	27.523±0.255	67.0	10.7±0.2
$>$1.4 (I)	58.33±1.19	57.40±1.06	79.8	10.66±0.29
$>$1.4 (II)	16.89±0.43	17.07±0.38	55.7	10.25±0.34
$>$1.4 (III)	6.21±0.43	7.73±0.48	51.2	6.44±0.60
$>$1.4 (IV)	42.2±1.7	39.1±1.5	82.6	11.45±0.63

Table 3: Observed number of muon candidates per hadronic event in the data and in the Monte Carlo and the corresponding BR's with the statistical errors are given for different p_t values. For the Monte Carlo the estimated purity of correctly identified semileptonic b–decays with an input BR of 10.45% is also given. The corresponding numbers for the high p_t muon candidates are also given separately for the two years of data taking and for the subsamples I–IV.

3.3 BR measurements with neutrinos

For the BR measurement with neutrinos, the missing energy spectrum of the jets in the lifetime tagged events, sample I, with a b–flavor purity of (59.4±1.5)% is used. With the requirement that the measured polar angle of the jet fulfills the condition $|\cos\theta_{\mathrm{Jet}}| < 0.65$, about 81000 jets are analyzed.

The measured missing energy spectrum is used to extract either BR(b$\rightarrow \nu X$) or BR(b$\rightarrow \tau\nu X$). The Monte Carlo neutrino spectrum for each semileptonic decay is found with the assumption of a V–A×V–A b–hadron decay structure. For the BR(b$\rightarrow \nu X$) measurement the neutrino spectrum is obtained from the combination of the different semileptonic b–hadron decays, assuming that the b–decay rate for the charged leptons (e:μ:τ) of 1:1:0.25±0.05, in agreement with different theoretical estimates [13]. Alternatively, the BR(b$\rightarrow e(\mu)\nu X$) is constrained and the excess is associated with the BR(b$\rightarrow \tau\nu X$).

To be as much as possible independent from the Monte Carlo, the background in the missing energy spectrum is determined from the data itself. This background is from jets with purely hadronic b–decays and from the remaining background from light quark flavored jets. The background determination uses the constraint that the jet energy spectra of the two–jet event sample (b–flavor purity of 22.8%) and the lifetime tagged b–flavor enriched event sample I (b–flavor purity of 59.4 ± 1.5%) have to be described simultaneously with the same inclusive branching ratio for $b \rightarrow \nu X$.

This method of estimating the background has been developed and tested with the Monte Carlo. Using different input semileptonic b–decay branching ratios and b–flavor purities, the background from mismeasured jets is found to be accurately described with this method. An example for this background description in the Monte Carlo is shown in figure 7, where the true background in sample I is shown together with the background estimated from the two–jet Monte Carlo events. The background is accurately described over the entire visible jet energy spectrum. It is found that with a known purity of the selected event samples, the MC input branching ratio BR(b$\rightarrow \nu X$) can be determined with a relative systematic accuracy of better than $\pm 2\%$.

Using a maximum likelihood fit to the two–jet sample and the subsample I to describe the jet energy spectra a BR($b \rightarrow \nu X$) of (23.08$\pm$0.77(stat.)$\pm$1.24(syst.))% is obtained. The jet energy spectrum from sample I and the result of the fit are shown in figure 8.

The systematic error is obtained by adding the different uncertainties in quadrature. In addition to the systematic error introduced by the method to determine the background, $\pm$0.61%, the error due to the b–flavor purity uncertainty of sample I, $\pm$0.90%, the uncertainties of the assumed neutrino energy spectra (this includes uncertainties due to the b–fragmentation function), $\pm$0.56%, and the uncertainty of the contribution from the BR(b$\rightarrow \tau\nu X$), $\pm$0.20%, are found to be important.

The uncertainty of the neutrino energy scale error ($\pm$200 MeV) and the resulting neutrino energy spectra has been estimated from our recent measurement of the average neutrino energy energy in events with observed electron and muon candidates [8] and from the modeling of semileptonic charm decays and of b$\rightarrow \tau\nu X$ decays.

To compare the semileptonic BR result obtained with neutrinos with the ones from electrons and muons the BR(b$\rightarrow \nu X$) has to be divided by 2.25. The result for BR(b$\rightarrow e(\mu)\nu X$) obtained from the neutrino measurement is (10.26$\pm$0.34(stat.)$\pm$0.55(syst.))%. This result has comparable errors to the direct measurements with electrons and muons. The agreement with the direct BR results obtained with electrons and muons indicates a consistent treatment of the energy spectra of the charged leptons and the corresponding neutrinos. It provides further evidence for parity violation due to the V–A structure in b–decays. In the case of a V+A b–decay structure, the average neutrino energy would be about 1.5 GeV larger. As a result of the wrong efficiency estimate, an apparent BR of 27$\pm$1% would have been seen in the case of a V+A b–decay structure. A value which is excluded from the neutrino BR measurement.

Assuming that the BR for electrons and muons is known with a certain accuracy, one can determine alternatively the additional contribution to the missing energy spectrum from the decay $b \rightarrow \tau\nu X$. To reduce the systematic error of the measurement, we use our directly measured BR's with electrons and muons.

Using the same method as above to determine the background, and the directly measured BR's with an average of (10.85$\pm$0.12$\pm$0.47)% with electrons and muons the result for the BR($b \rightarrow \tau\nu X$) is: (1.67$\pm$0.46(stat.)$\pm$1.04(syst.))%. The jet energy spectrum and the result of the fit are shown in figure 9.

The systematic error comes from the above error on the electron and muon BR's, $\pm$0.79%, the error of the background estimation, $\pm$0.33%, the assumed $\pm$200 MeV energy scale uncertainty in the missing energy spectrum, $\pm 0.43\%$, and the b–flavor purity of sample I $\pm 0.53\%$

This result is in good agreement with the assumptions used to determine the inclusive neutrino BR and the theoretical estimates for the ratio BR(b$\rightarrow$ $\tau\nu X$)/BR(b$\rightarrow$ $e^{\pm}\nu X$). This result is compared in figure 10 with other measurements of the semileptonic BR with τ's [14] and [15] and also with the theoretical estimates [13]. One concludes that consistent results between the data and the predictions are obtained for a semileptonic BR(b$\rightarrow$ $e\nu X$) of 10.5$\pm$0.5%.

4 Discussion of the results

The semileptonic BR(b$\rightarrow$ $e(\mu)\nu X$) has been measured with inclusive electrons and muons assuming the ACCM spectra with a polarization of the W with a V–A structure. The different measurements are found to be consistent within the errors and can be combined, giving an average BR(b$\rightarrow$ $e(\mu)\nu X$) value of (10.85$\pm$0.12$\pm$0.47)%.

Using the independent neutrino BR measurement and taking the correlations of the different systematic errors into account, one obtains a combined BR(b$\rightarrow$ $e(\mu)\nu X$) of (10.73$\pm$0.11$\pm$0.46)%.

This BR value agrees with the model independent measurements from ARGUS and CLEO[16] and is about 10% lower than our previous result, obtained using inclusive electrons and muons [1] using from the 1990 and 1991 data sample.

The origin of this difference has been investigated. About half of the difference is explained by the harder b–hadron fragmentation function, used in this analysis with an average energy of 72$\pm$2% (instead of 68$\pm$2%) of the beam energy. This energy increase was required in order to match the measured charged lepton energy spectra from the two–jet analysis with the Monte Carlo.

The remaining difference of 5% could originate from the two–jet analysis, which was not applied in our previous analysis. Since the charged lepton analysis depends on the assumed p and p_t spectra of the weakly decaying b–hadrons, such a possibility seems likely. Differences in the collinear gluon radiation from b–quarks and light quarks, which would alter the and thus the predicted p_t spectra for b–flavored hadrons, have been discussed for example in reference [17].

To study these possible b–quark mass effects in more detail, the data sample of well measured hadronic events is subdivided into five different subsamples. For this selection the mass obtained from all calorimeter clusters found in one hemisphere is determined. The larger mass of the two hemispheres defines the "fat" jet. The subsamples are selected according to the observed mass of the "fat" jet. The data and Monte Carlo mass distributions are shown in figure 11a. The average mass of the "fat jet" is about 500 MeV larger in the data than in the Monte Carlo. The ratio between the data and Monte Carlo mass distributions is shown in figure 11b. The fraction of events with a mass below 10 GeV, is 20% less in the data than in the Monte Carlo. A similar depletion of low jet masses is observed for the "thin" jet.

The flavor content of events falling into the five different "fat jet" classes is investigated using the fraction of events which are classified into subsamples I–III and also from the fraction of high p_t inclusive electron and muon candidates. A clear systematic trend in opposite directions is found for b–flavor enriched and b–flavor depleted events. The observed b–flavor content increases in the data relative to the Monte Carlo from about 90% for low jet masses to about 130% for high jet masses. At the same time, the fraction of light flavor events is found to decrease. Consequently, the "apparent" semileptonic BR depends on the fraction of b–flavored jets in the selected subsamples. Taking the Monte Carlo predictions for the b–purity of jets found within the selected mass region of the "fat jet", the apparent BR values are unstable, as shown in table 4 for electrons and muons.

Taking the difference between the lifetime tagged events sample I and sample II in the data and the Monte Carlo the b–purity from the Monte Carlo can be corrected for the different mass bins of the fat–jet. With this correction for the b–flavor purity, reasonably stable apparent semileptonic BR's (statistical error only!) are obtained for electrons and muons, as given in table 4.

Using this correction method and combining the different subsamples a semileptonic BR for the entire two– and three-jet event sample of 10.6±0.2% using electrons and 10.8±0.14% is obtained. These values are in agreement with the measured BR result obtained from the two–jet event sample (section 3.1 and 3.2). As this effect of the jet–mass is not completely understood, the differences between the BR result from the two jet analysis and the combined BR's obtained with this correction, as given in table 2, are added to the systematic errors of the BR measurement.

	Electrons			Muons		
$m_{fat-jet}$ (GeV)	n_e	app. BR	corr. app. BR	n_μ	app. BR	corr. app. BR
–10.	673	8.8±0.4	10.0±0.5	1248	9.5±0.3	10.7±0.4
10.–15.	2494	10.5±0.3	10.4±0.3	4609	10.5±0.2	10.4±0.2
15.–20.	1547	11.5±0.4	10.6±0.4	2903	11.2±0.3	10.5±0.3
20.–25.	771	12.1±0.6	11.3±0.6	1320	11.7±0.5	11.0±0.5
$>$ 25.	657	13.4±0.8	11.2±0.7	1137	14.0±0.6	12.2±0.5

Table 4: Observed number of events with high p_t electron (n_e) or muon candidates (n_μ) for $p_t > 1.4$ GeV and for the different mass bins in the data and the the apparent BR using the b–flavor fraction as found in the Monte Carlo and corrected using the b–flavor fraction per mass bin from sample I and II. For numbers only the statistical errors are given.

The difference between the modeling of b–flavored jets and the data is found to be the most likely explanation for the 10% lower BR with our new measurement. Even though, other interpretations are possible, the difference between light quark flavored jets and b–flavored jets could lead to an explanation of the current discrepancy between previously published semileptonic BR measurements from LEP, and the measurements at the $\Upsilon(4S)$ resonance [18].

5 Summary

The semileptonic branching ratio BR($b \to \ell^{\pm}\nu X$) has been measured with electrons, muons and neutrinos using a two–jet hadronic event sample. The efficiency and backgrounds have been cross checked with b–enriched and b–depleted event subsamples.

The results obtained for the BR are:

$$\mathbf{BR(b\to} \, e\nu X\mathbf{)} = \mathbf{(10.89 \pm 0.20 \pm 0.51)\%},$$

$$\mathbf{BR(b\to} \, \mu\nu X\mathbf{)} = \mathbf{(10.82 \pm 0.15 \pm 0.5)\%},$$

$$\mathbf{BR(b\to} \, \nu X\mathbf{)} = \mathbf{(23.08 \pm 0.77 \pm 1.26)\%}.$$

For the neutrino BR measurement it has been assumed that the different charged leptons (e:μ:τ) from semileptonic b–decays are produced in the ratio of 1:1:0.25±0.05. The neutrino result divided by 2.25 then gives in a value of:

$$\mathbf{BR(b\to} \, e(\mu)\nu X\mathbf{)} = \mathbf{(10.26 \pm 0.34 \pm 0.55\%)}.$$

Combining these three measurements and taking correlation into account one obtains:

$$\mathbf{BR(b\to} \, e(\mu)\nu X\mathbf{)} = \mathbf{(10.73 \pm 0.11 \pm 0.46\%)}.$$

Using alternatively the results of our direct measurement for the BR(b$\to e(\mu)\nu X$) as a constraint, the BR(b$\to \tau\nu X$) and the ratio R = BR(b$\to \tau\nu X$)/BR(b$\to e\nu X$) are measured to be:

$$\mathbf{BR(b\to} \, \tau\nu X\mathbf{)} = \mathbf{(1.67 \pm 0.46 \pm 1.04\%)}.$$

$$\mathbf{R = 0.154 \pm 0.042 \pm 0.072}.$$

This new BR result agrees with theoretical estimates for a BR(b$\to e\nu X$) of 10.5±0.5%.

References

[1] L3 Collaboration, L3 Note 1625 results for the Glasgow conference, ICHEP94 (1994).

[2] L3 Collaboration, B. Adeva et al., Nucl. Inst. and Meth. **A289** (1990) 35.

[3] L3 Collaboration, B. Adeva *et al.*, Z. Phys. **C51** (1991) 179.

[4] T. Sjöstrand, Comput. Phys. Commun. **27** (1982) 243; and PYTHIA 5.6 and JETSET 7.3.

[5] The L3 detector simulation is based on GEANT Version 3.14; see R. Brun *et al.*, GEANT 3, CERN DD/EE/84-1 (Revised), September 1987 and the GHEISHA program (H. Fesefeld, RWTH Aachen Report PITHA85/02 (1985) for the simulation of hadronic interactions.

[6] Particle Data Group, L. Montanet *et al.*, Phys. Rev. **D50**(1994) 1173;
DELCO Collaboration, W. Bacino *et al.*, Phys. Rev. Lett. **43** (1979) 1073 and
MARK III Collaboration, R. M. Baltrusaitis *et al.*, Phys. Rev. Lett. **54** (1985) 1976.

[7] G. Altarelli *et al.*, Nucl. Phys. **B208** (1982) 365.

[8] L3 Collaboration, M. Acciarri et al. Phys. Lett. **B351** (1995) 375.

[9] C. Peterson *et al.*, Phys. Rev.**D27** (1983) 105.

[10] The LEP Collaborations, CERN/PPE/94-187 (25 November 1994)

[11] N. Isgur *et al.*, Phys. Rev.**D39** (1989) 799. CERN/PPE/94-187 (25 November 1994)

[12] See for example R. H. Schindler page 1602 in Particle Data Group, L. Montanet *et al.*, Phys. Rev. **D50**(1994) 1173.

[13] P. Heiliger and L. M. Sehgal, Phys. Lett. **B229** (1989) 409., and
A. Falk *et al.*, Phys. Lett. **B326**(1994) 145.

[14] ALEPH Collaboration, D. Buskulic *et al.*, Phys. Lett. **B343** (1995) 444.

[15] L3 Collaboration, M. Acciarri *et al.*, Phys. Lett. **B332**(1994) 201.

[16] ARGUS collaboration, H. Albrecht et al., Phys. Lett. **B318** (93) 397 and
CLEO collaboration., CLEO–Conf 94–6.

[17] See for example Y. L. Dokshitzer et al., Basics of QCD, ed. Tran Than Van, Editions Frontieres, Paris, 1991.

[18] See for example J. R. Patterson, Proceedings of the 27th international Conf. on High Energy Physics, Glasgow 1994, 149.

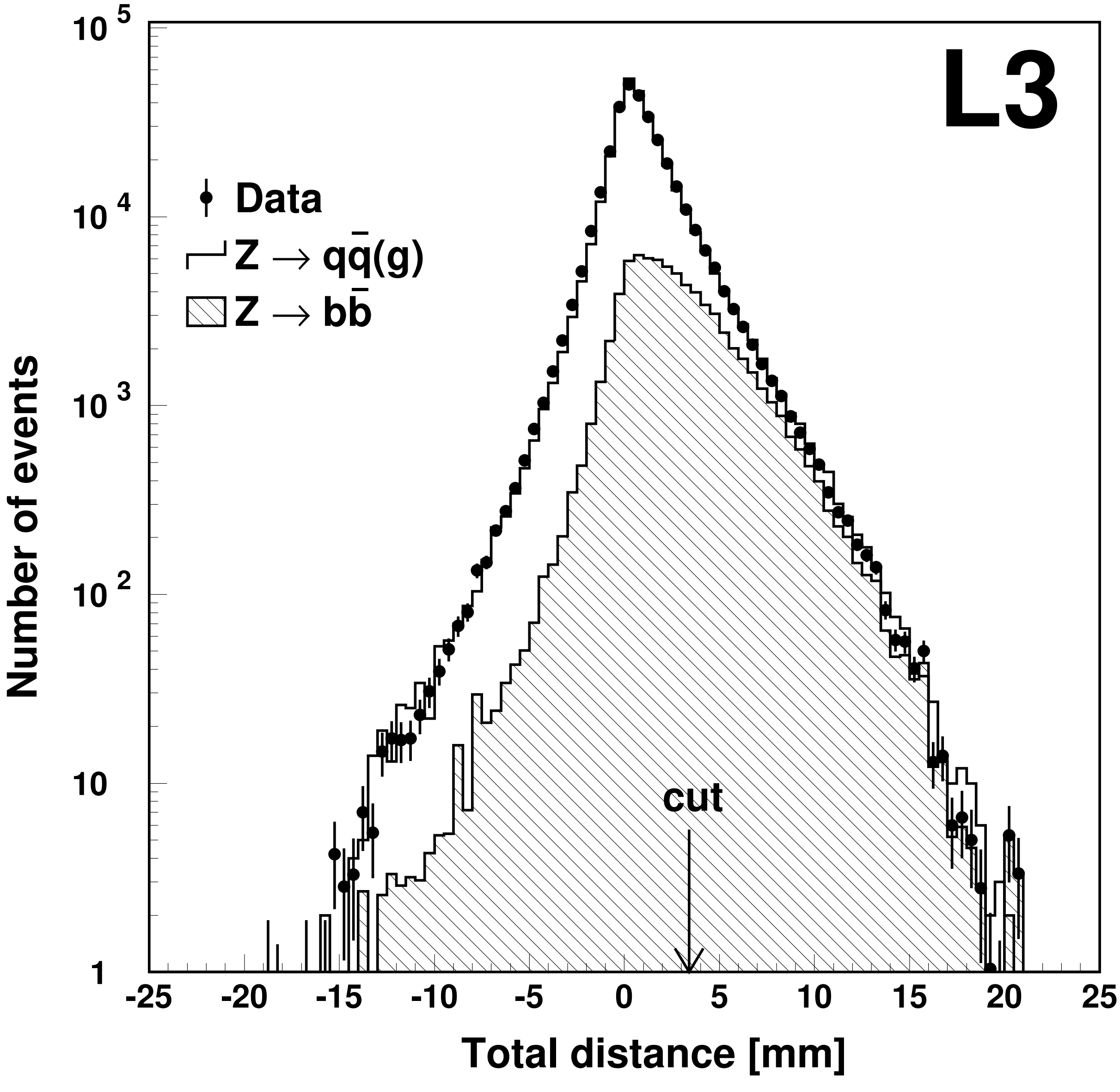

Figure 1: Measured distance between the two reconstructed jet vertices in data and Monte Carlo. Sample I are the events with a distance of more than 3.5 mm. The estimated fraction of b–flavored events is also shown.

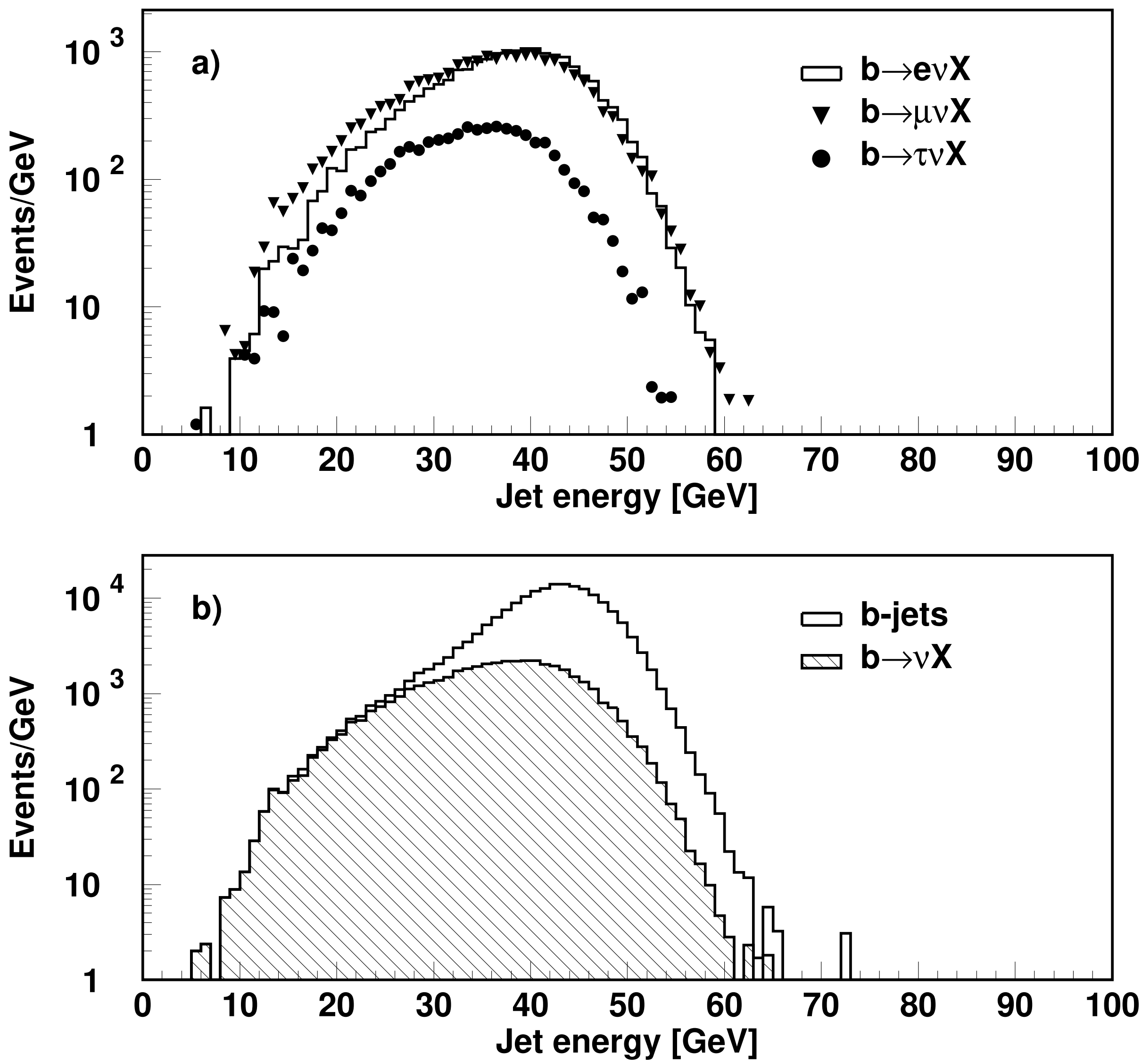

Figure 2: The visible energy spectrum of jets in the Monte Carlo from the different semileptonic b–decays (a). The visible energy spectrum of Monte Carlo b–flavored jets together with the contribution from semileptonic b–hadron decays is shown in (b).

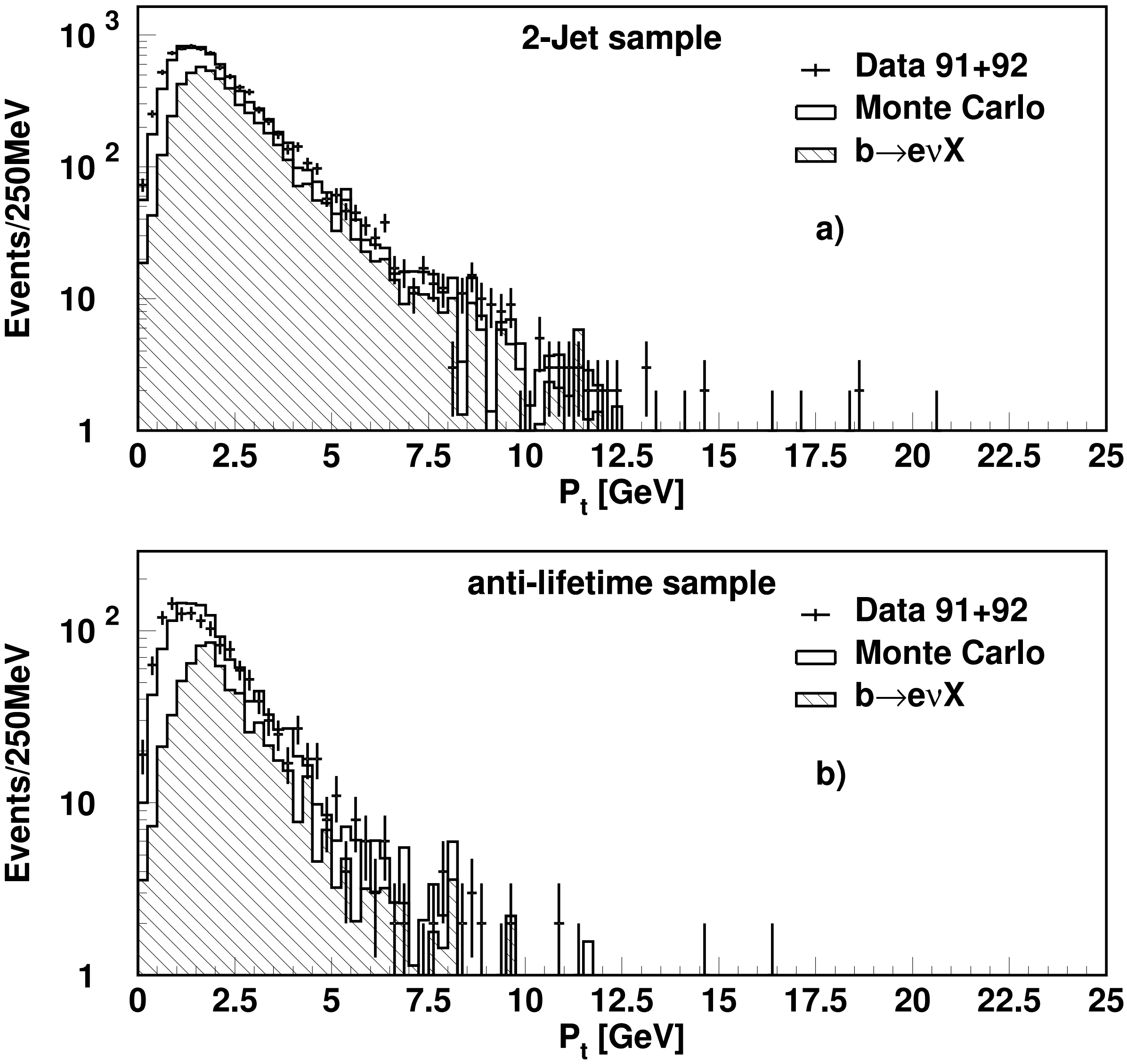

Figure 3: The p_t spectrum with respect to the jet direction for the electron candidates in the two–jet sample (a) and in the b–depleted sample II (b). The corresponding Monte Carlo distributions are also shown together with the fraction of correctly identified semileptonic b–decays.

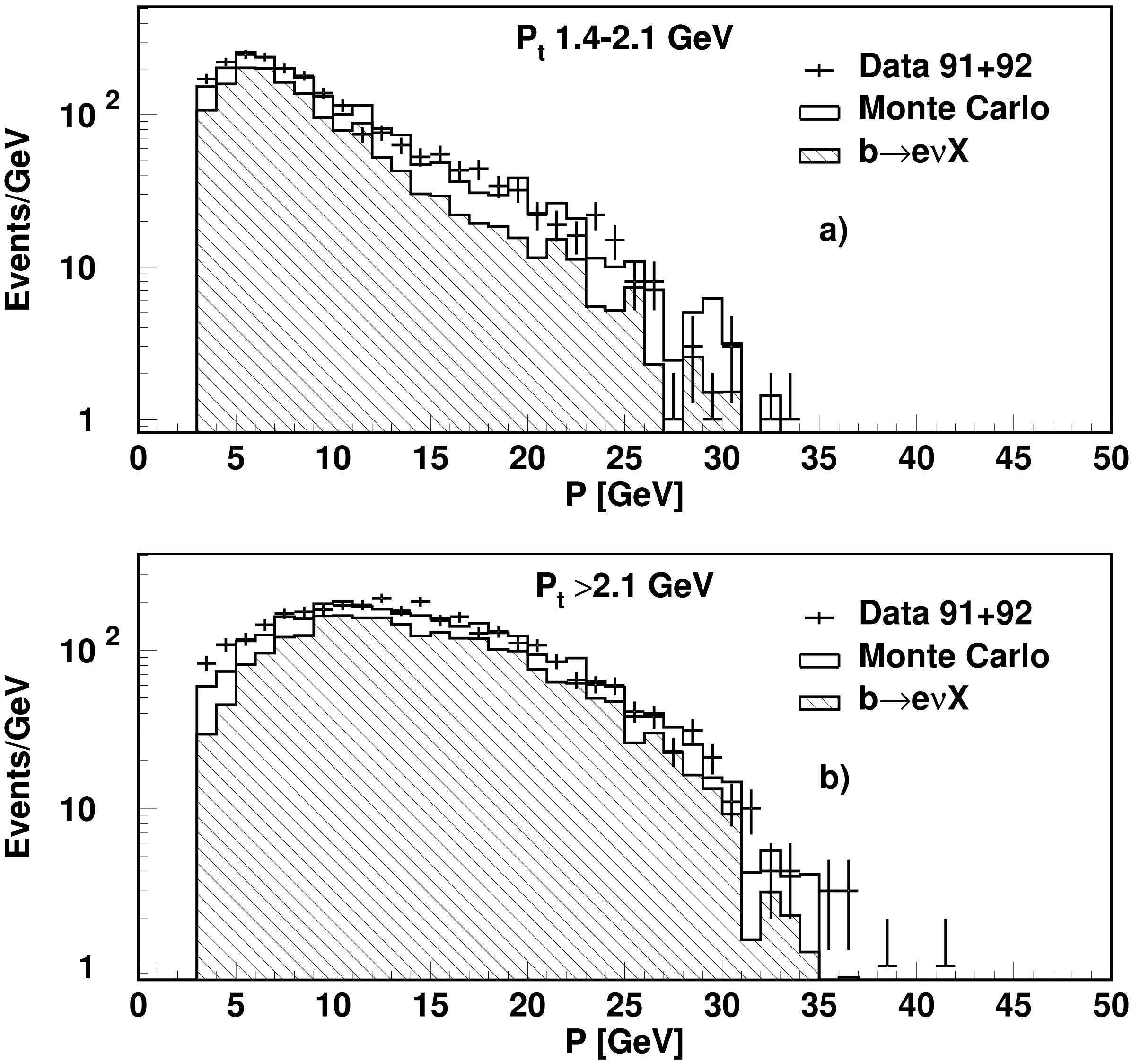

Figure 4: The p spectrum of the electron candidates with a p_t with respect to the jet direction between 1.4–2.1 GeV (a) and and for p_t values of more than 2.1 GeV (b). The corresponding Monte Carlo distributions are also shown together with the fraction of correctly identified semileptonic b–decays.

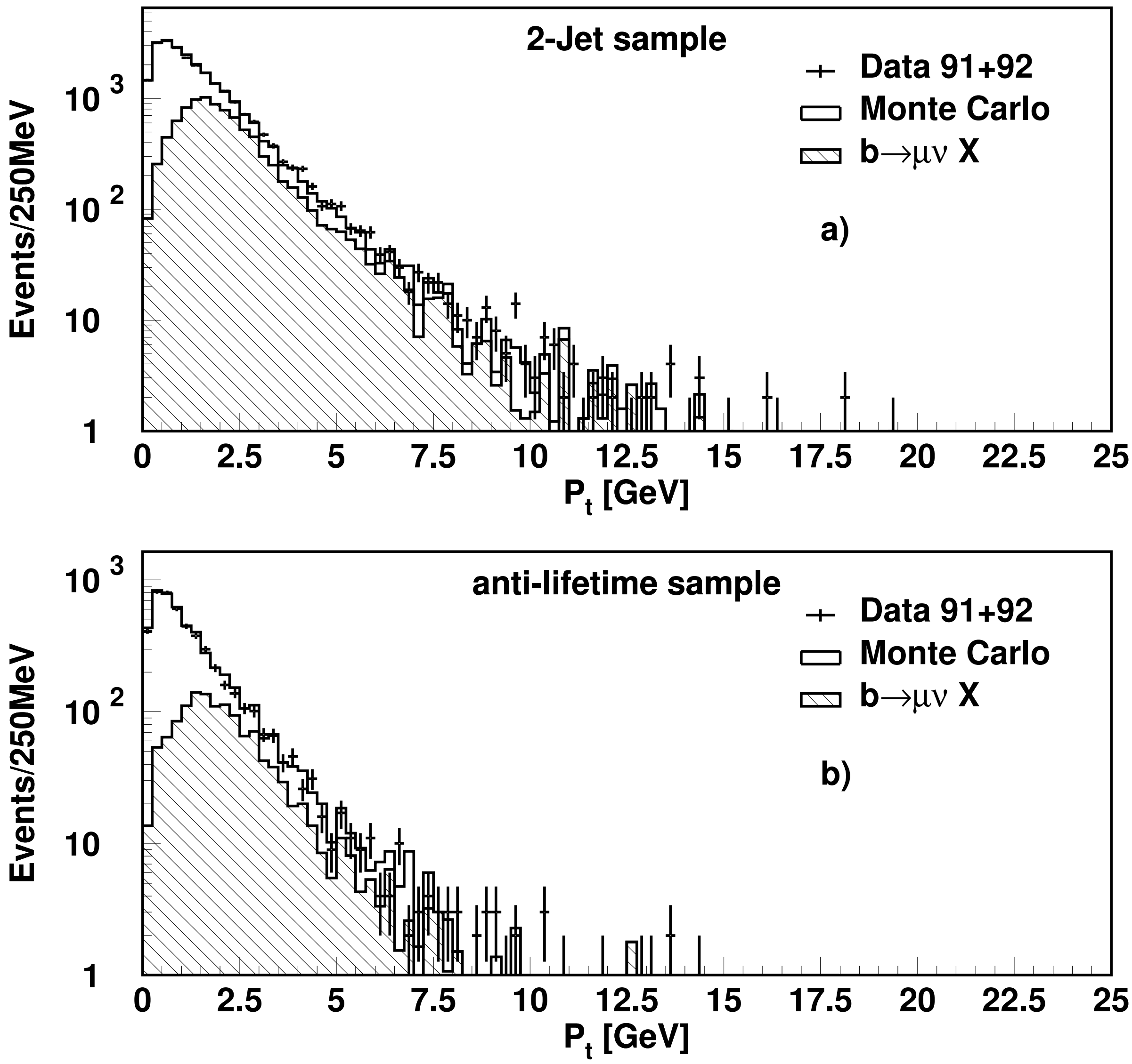

Figure 5: The p_t spectrum with respect to the jet direction for the muon candidates in the two–jet sample (a) and in the b–depleted sample II (b). The corresponding Monte Carlo distributions are also shown together with the fraction of correctly identified semileptonic b–decays.

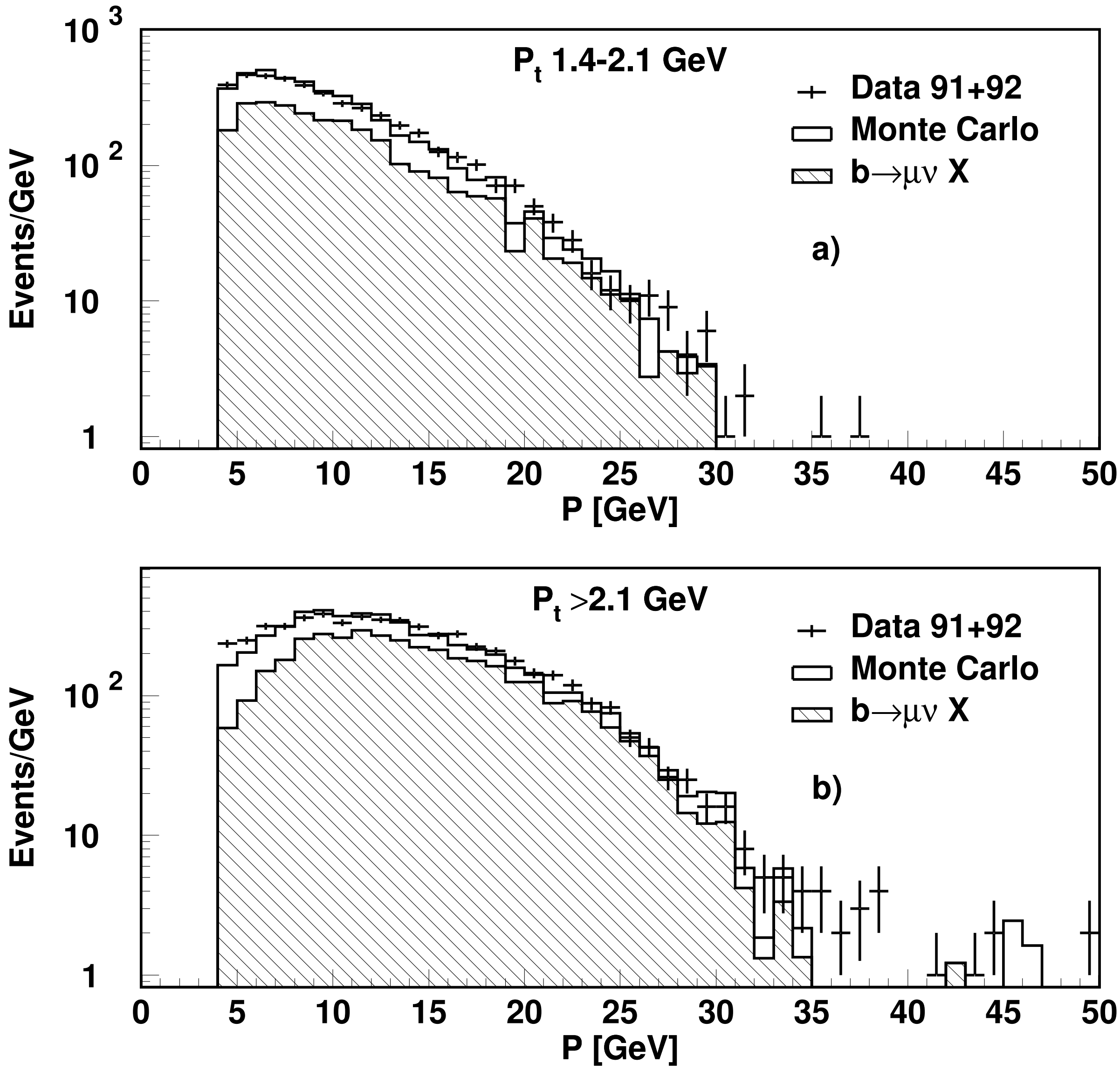

Figure 6: The p spectrum of the muon candidates with a p_t with respect to the jet direction between 1.4–2.1 GeV (a) and and for p_t values of more than 2.1 GeV (b). The corresponding Monte Carlo distributions are also shown together with the fraction of correctly identified semileptonic b–decays.

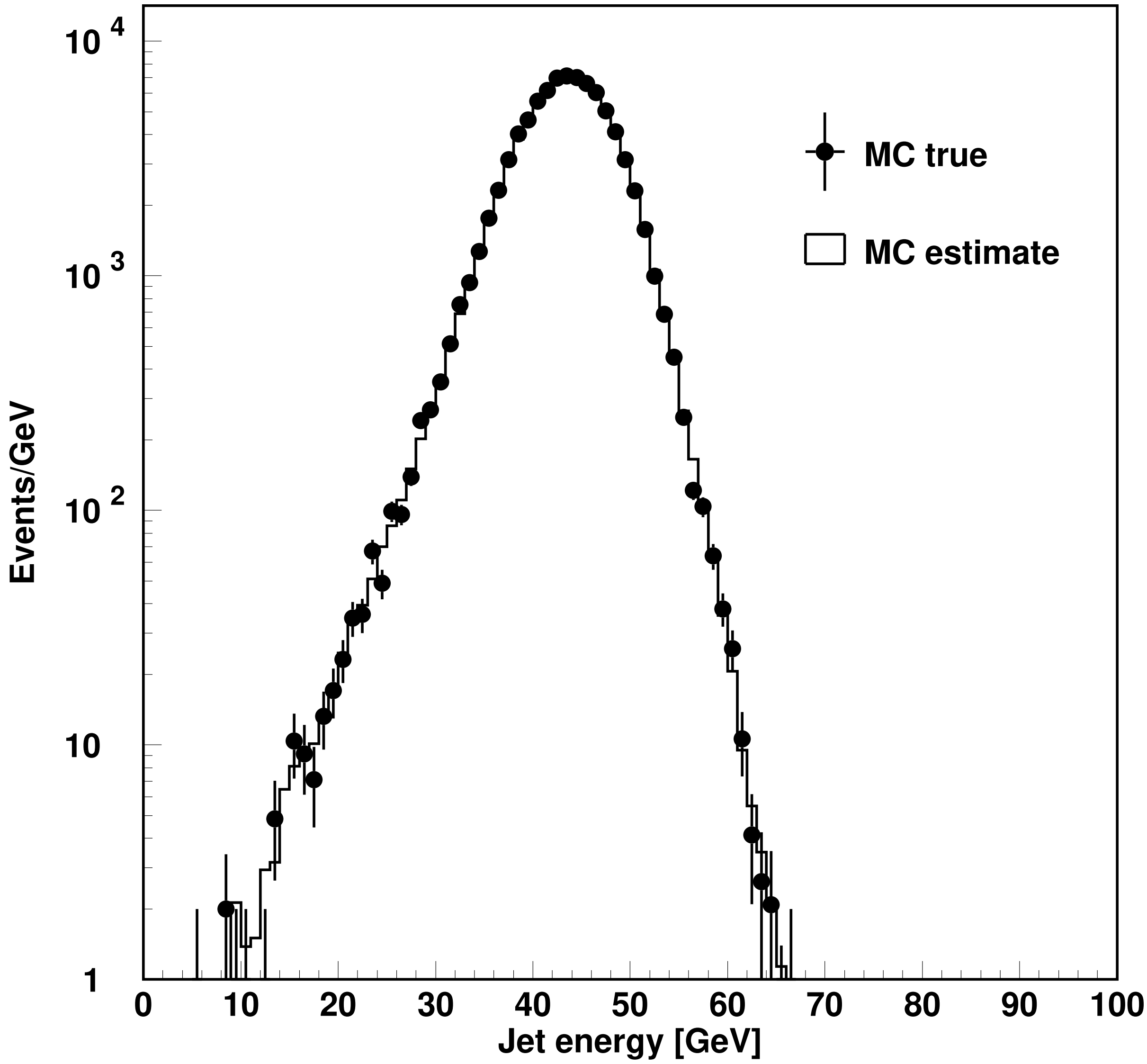

Figure 7: The Monte Carlo jet energy distribution for the true hadronic background in sample I and the estimated background from the Monte Carlo two–jet sample.

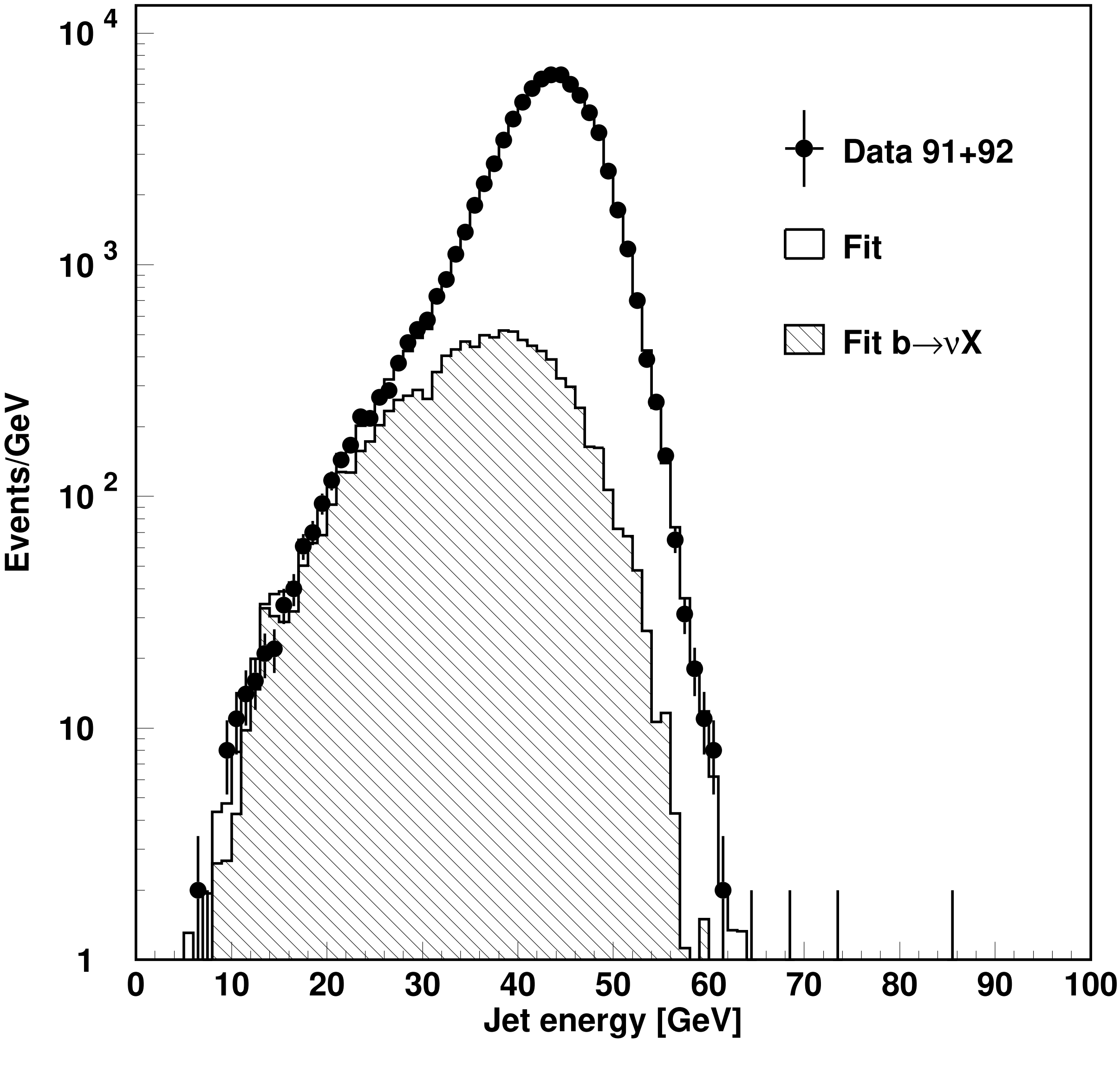

Figure 8: The jet energy spectrum of sample I in the data and the results of the fit for the measurement of BR(b$\rightarrow \nu X$).

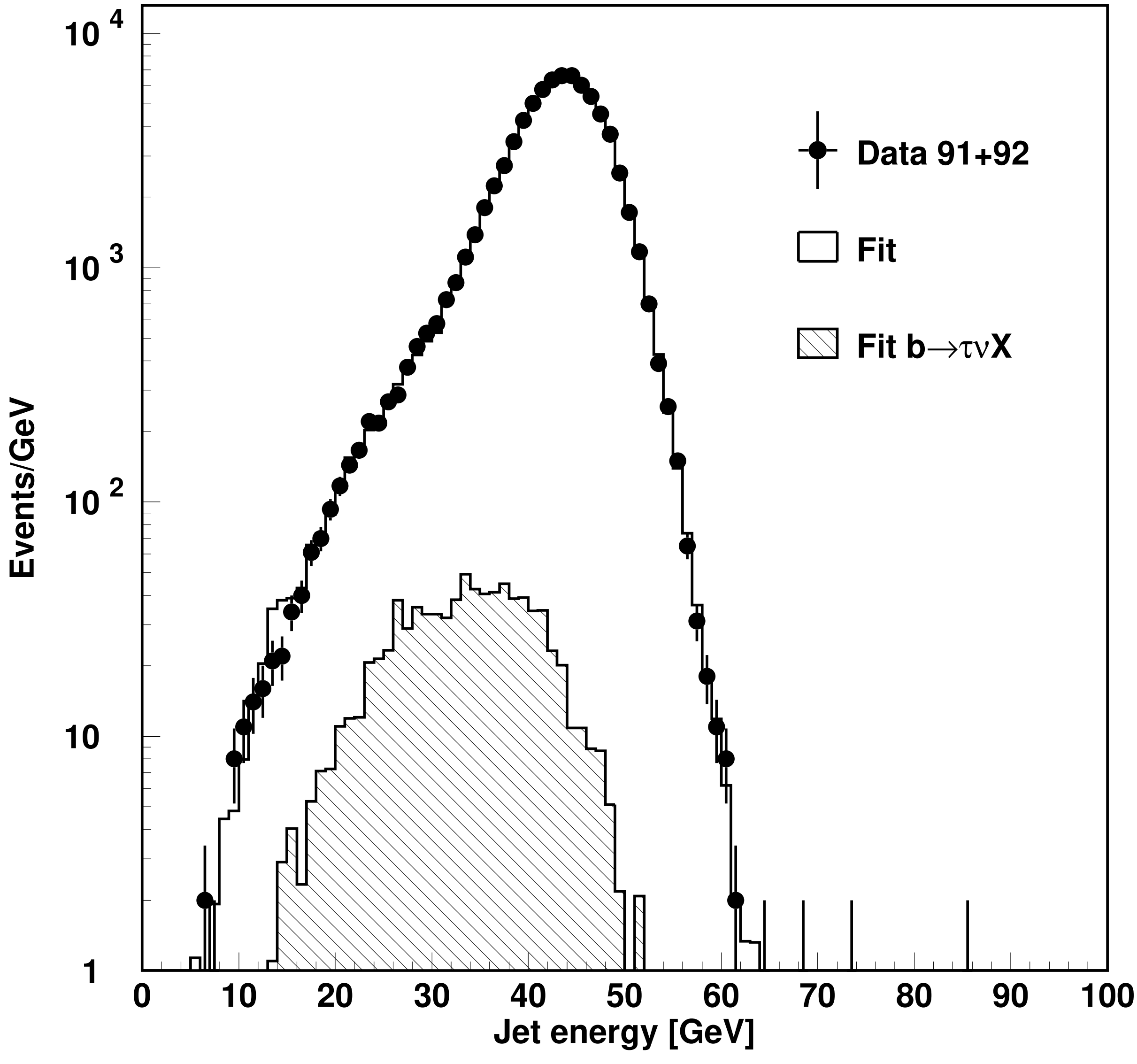

Figure 9: The jet energy spectrum of sample I in the data and the results of the fit for the measurement of BR(b→ $\tau\nu X$) with the constrained BR(b→ $e(\mu)\nu X$) of 10.85%.

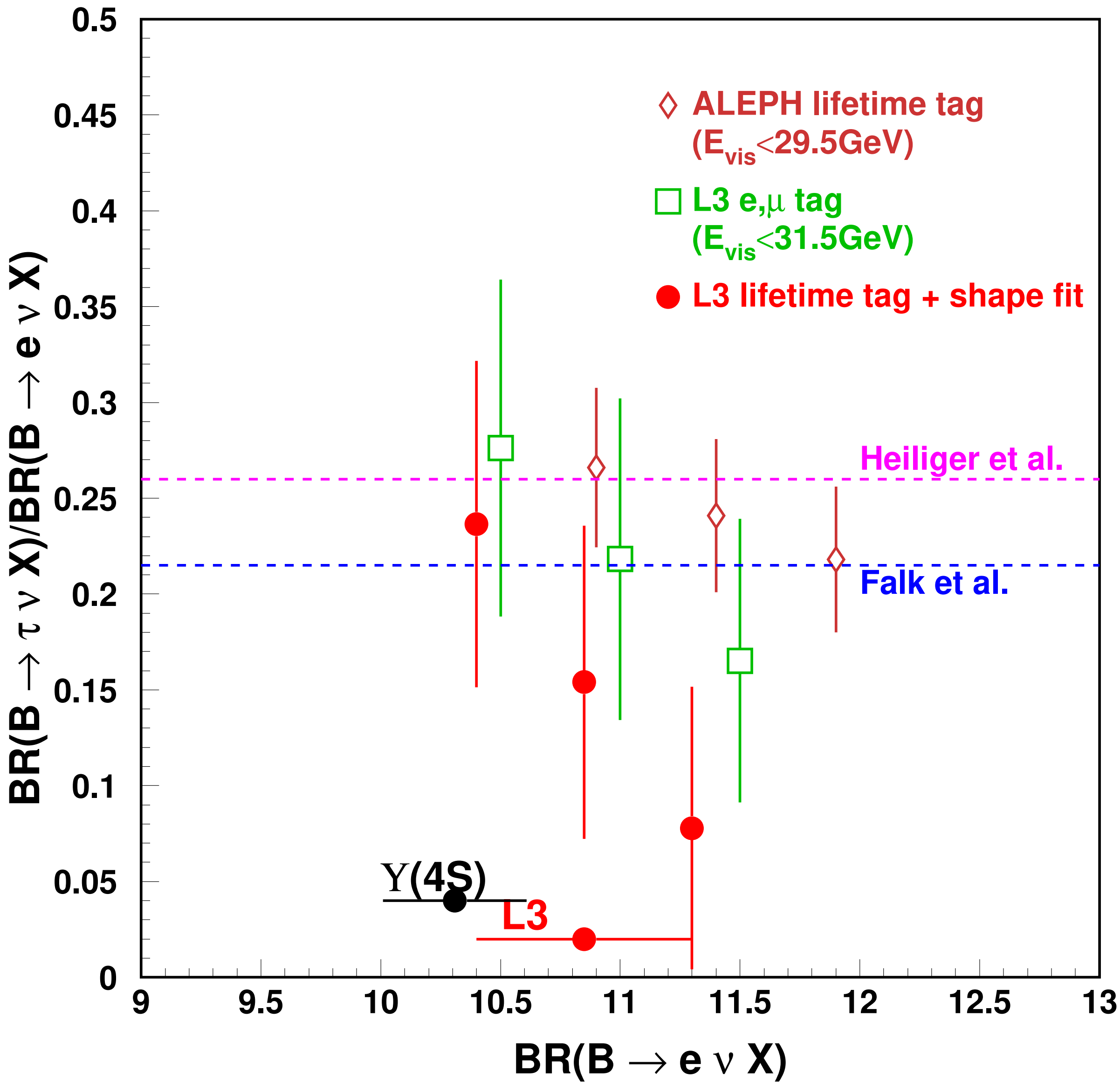

Figure 10: Compilation of different measurements for the ratio of the BR(b→ $\tau\nu X$)/BR(b→ $e\nu X$) as a function of the BR(b→ $e\nu X$). The results from our direct measurement for BR(b→ $e\nu X$) and the average BR result from the Υ(4S) experiments [18] are also shown.

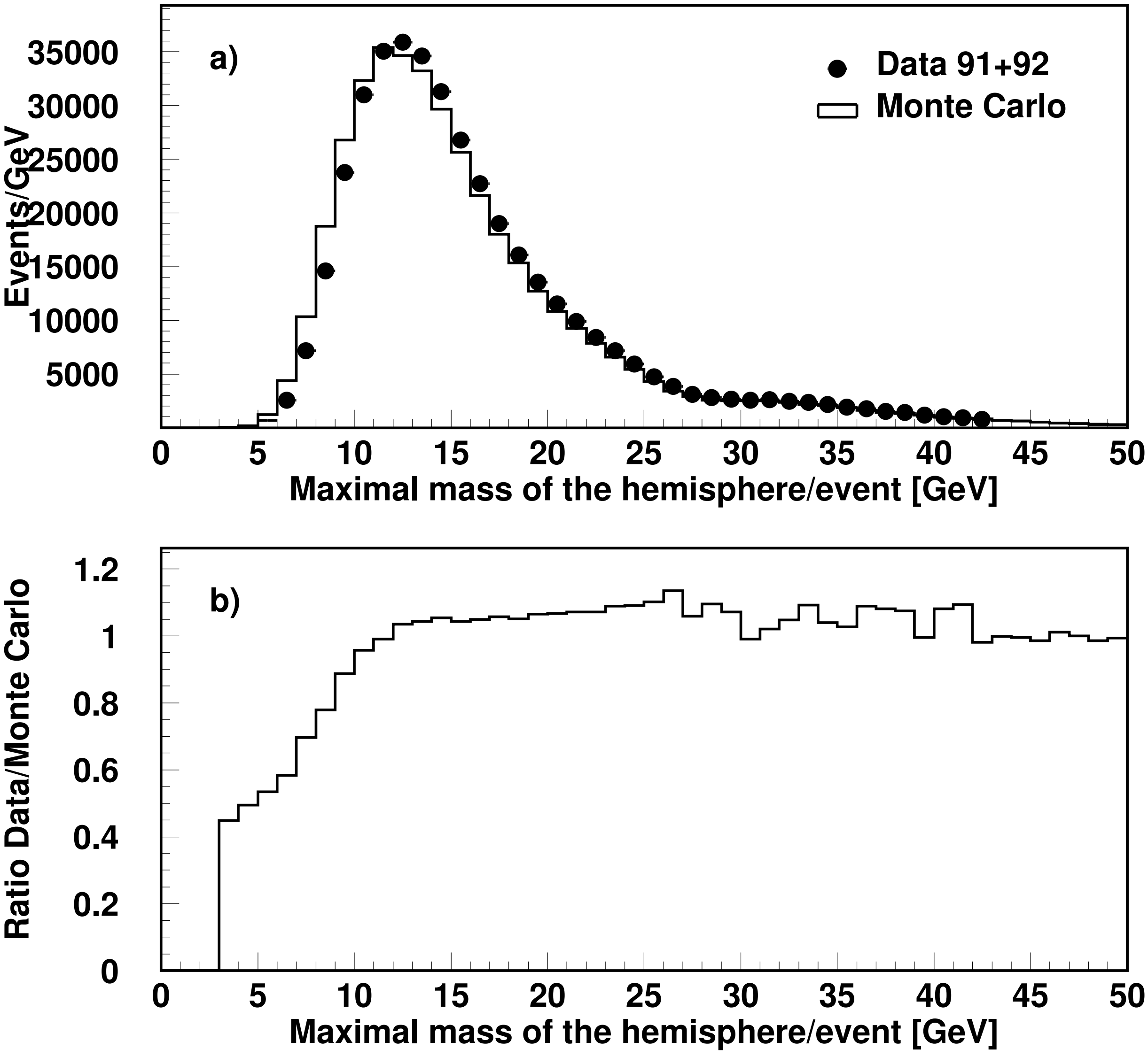

Figure 11: The distribution of the maximal hemisphere mass per event in data and in Monte Carlo (a) and (b) the ratio of the two distributions.